

Robust PSSE Using Graph Neural Networks for Data-driven and Topology-aware Priors

Qiuling Yang, Alireza Sadeghi, Gang Wang, Georgios B. Giannakis, *Fellow, IEEE*, and Jian Sun

Abstract—Distributed renewable generation, elastic loads, and purposeful manipulation of meter readings challenge the monitoring and control of today’s power systems (PS). In this context, to maintain a comprehensive view of the system in real time, fast and robust state estimation (SE) methods are urgently needed. Conventional PSSE solvers typically entail minimizing a nonlinear and nonconvex least-squares by e.g., the workhorse Gauss-Newton method. Those iterative solvers however, are sensitive to initialization and may get stuck in local minima. To overcome these hurdles and inspired by recent image denoising techniques, this paper advocates a learnable regularization term for PSSE that uses a deep neural network (DNN) prior. For the resultant regularized PSSE problem, a “Gauss-Newton-like” alternating minimization solver is first developed. To accommodate real-time monitoring, a novel end-to-end DNN is constructed by unrolling the proposed alternating minimization solver. Interestingly, the power network topology can be easily incorporated into the DNN by designing a graph neural network (GNN) based prior. To further endow the physics-based DNN with robustness against bad data, an adversarial DNN training method is discussed. Numerical tests using real load data on the IEEE 118-bus benchmark system showcase the improved estimation and robustness performance of the proposed scheme compared with several state-of-the-art alternatives.

Index terms— State estimation, deep prior, graph neural network, robust optimization.

I. INTRODUCTION

In today’s smart grid, reliability and accuracy of state estimation are central for several system control and optimization tasks, including optimal power flow, unit commitment, economic dispatch, and contingency analysis [2]. However, frequent and sizable state variable fluctuations caused by fast variations of renewable generation, increasing deployment of electric vehicles, and human-in-the-loop demand response, are challenging these functions.

As state variables are difficult to measure directly, the supervisory control and data acquisition (SCADA) system offers abundant measurements, including voltage magnitudes, power flows, and power injections. Given SCADA measurements, the goal of PSSE is to retrieve the state variables, namely complex voltages at all buses [2]. PSSE is typically formulated

as a (weighted) least-absolute-value (WLAV) or a least-squares (WLS) problem, both of which are ill-posed, and nonconvex in general [31].

To address these challenges, several efforts have been devoted. For example, the LAV estimation problem was converted into a constrained optimization, for which a sequential linear programming solver was devised in [13], and improved (stochastic) proximal-linear solvers were developed in [29]. On the other hand, focusing on the WLS problem, the Gauss-Newton solver is widely employed in practice [2]. Unfortunately, due to the nonconvexity and quartic loss function, there are two issues in implementing the Gauss-Newton solver: i) sensitivity to initialization; and ii) no convergence guarantee in general [38]. Semidefinite programming approaches can mitigate these issues to some extent, but they incur a heavy computational burden [38]. In a nutshell, the grand challenge of these methods, remains to develop fast and robust PSSE solvers attaining or approximating the global optimum.

To bypass the nonconvex optimization hurdle, recent works have focused on developing data- (and model-) driven neural network (NN) solutions [5], [20], [37], [36], [35], [8], [33], [12], [34], [24], [9]. Such NN-based PSSE solvers aim at directly approximating the mapping from measurements to state variables based on a training set of measurement-state pairs generated using simulators or available from historical data [36]. Unfortunately, these NN architectures are not effective in exploring the power network topology. On the other hand, a common approach to tackling challenging ill-posed problems in image processing has been to regularize the loss function with appropriate priors [25]. Popular priors include sparsity, total variation, and low-rank penalty [10]. Recent efforts have also focused on data-driven priors that can be learned from exemplary data [18], [26], [3].

Building on [26], [3], this paper advocates a deep (D) NN-based trainable prior for standard ill-posed PSSE, to promote physically meaningful PSSE solutions. To tackle the resulting regularized PSSE problem, an alternating minimization-based solver is first developed, which entails Gauss-Newton iterations as a critical algorithmic component. As with Gauss-Newton iterations, our solver requires inverting a matrix per iteration, incurring a heavy computational burden that discourages it from real-time system monitoring. To accommodate real-time operations and building on our previous works [37], [36], we unroll this alternating minimization solver to construct a new DNN architecture, called unrolled Gauss-Newton with deep priors (GN-DP). As the name suggests, our DNN model consists of a Gauss-Newton iteration as a basic building block, followed by a proximal step to account for

The work of Q. Yang and J. Sun was supported in part by NSFC Grants 61522303, 61720106011, and 61621063. Q. Yang was also supported by the China Scholarship Council. The work of A. Sadeghi, G. Wang, and G. B. Giannakis was supported by NSF grants 1711471 and 1901134. Q. Yang and J. Sun are with the State Key Lab of Intelligent Control and Decision of Complex Systems, School of Automation, Beijing Institute of Technology, Beijing 100081, China (e-mail: yang6726@umn.edu, sunjian@bit.edu.cn). A. Sadeghi, G. Wang, and G. B. Giannakis are with the Department of Electrical and Computer Engineering, University of Minnesota, Minneapolis, MN 55455, USA (e-mail: sadeghi@umn.edu, gangwang@umn.edu, georgios@umn.edu).

the regularization term. Interestingly, by means of employing a graph (G) NN-based prior, our model exploits the structure of the underlying power network. Different from [36], our GN-DP method offers a systematic and flexible framework to incorporate topology-aware prior information into standard PSSE tasks.

In practice, measurements collected by the SCADA system may be grossly corrupted due to e.g., parameter uncertainty, instrument mis-calibration, and unmonitored topology changes [21], [29]. As a cyber-physical system, power networks are also vulnerable to adversarial attacks [11], [32], as asserted by the first hacker-caused Ukraine power blackout in 2015 [7]. Furthermore, it has recently been demonstrated that adversarial attacks can severely deteriorate NNs' performance [16], [23]. Prompted by this, to endow our GN-DP scheme with *robustness* against bad data and even adversaries, we pursue a principled GN-DP training method through a distributionally robust optimization perspective. Numerical tests using the IEEE 118-bus benchmark system corroborate the estimation performance and robustness of the proposed scheme.

Paper outline. Regarding the remainder of the paper, Section II introduces the power system model and formally states the PSSE problem. Section III presents a general framework for incorporating data-driven and topology-aware priors into PSSE, and an alternating minimization solver for the resultant regularized PSSE, followed by the unrolled GN-GNN. Section IV develops a robust GN-GNN version. Numerical tests using the IEEE 118-bus test feeder are provided in Section V, with concluding remarks drawn in Section VI.

Notation. Lower- (upper-) case boldface letters denote column vectors (matrices), with the exception of vectors \mathbf{V} , \mathbf{P} and \mathbf{Q} , and normal letters represent scalars. The (i, j) entry, i -th row, and j -th column of matrix \mathbf{X} are $[\mathbf{X}]_{i,j}$, $[\mathbf{X}]_{i,:}$, and $[\mathbf{X}]_{:,j}$, respectively. Calligraphic letters are reserved for sets except operators \mathcal{I} and \mathcal{P} . Symbol $^\top$ stands for transposition; $\mathbf{0}$ denotes all-zero vectors of suitable dimensions; and $\|\mathbf{x}\|$ is the l_2 -norm of vector \mathbf{x} .

II. BACKGROUND AND PROBLEM FORMULATION

Consider an electric grid comprising N buses (nodes) with E lines (edges) that can be modeled as a graph $\mathcal{G} := (\mathcal{N}, \mathcal{E}, \mathbf{W})$, where the set $\mathcal{N} := \{1, \dots, N\}$ collects all buses, $\mathcal{E} := \{(n, n')\} \subseteq \mathcal{N} \times \mathcal{N}$ all lines, and $\mathbf{W} \in \mathbb{R}^{N \times N}$ is a weight matrix with its (n, n') -th entry $[\mathbf{W}]_{nn'} = w_{nn'}$ modeling the impedance between buses n and n' . In particular, if $(n, n') \in \mathcal{E}$, then $[\mathbf{W}]_{nn'} = w_{nn'}$; and $[\mathbf{W}]_{nn'} = 0$ otherwise. For each bus $n \in \mathcal{N}$, let $V_n := v_n^r + jv_n^i$ be its complex voltage with magnitude denoted by $|V_n|$, and $P_n + jQ_n$ its complex power injection. For reference, collect the voltage magnitudes, active and reactive power injections across all buses into the N -dimensional column vectors $|\mathbf{V}|$, \mathbf{P} , and \mathbf{Q} , respectively.

System state variables $\mathbf{v} := [v_1^r \ v_1^i \ \dots \ v_N^r \ v_N^i]^\top \in \mathbb{R}^{2N}$ can be represented by SCADA measurements, including voltage magnitudes, active and reactive power injections, as well as active and reactive power flows. Let \mathcal{S}_V , \mathcal{S}_P , \mathcal{S}_Q , \mathcal{E}_P , and \mathcal{E}_Q denote the sets of buses or lines where meters of

corresponding type are installed. For a compact representation, let us collect the measurements from all meters into $\mathbf{z} := [\{|V_n|^2\}_{n \in \mathcal{S}_V}, \{P_n\}_{n \in \mathcal{S}_P}, \{Q_n\}_{n \in \mathcal{S}_Q}, \{P_{nn'}\}_{(n,n') \in \mathcal{E}_P}, \{Q_{nn'}\}_{(n,n') \in \mathcal{E}_Q}]^\top \in \mathbb{R}^M$. Moreover, the ℓ -th entry of $\mathbf{z} := \{z_m\}_{m=1}^M$, can be described by the following model

$$z_m = h_m(\mathbf{v}) + \epsilon_m, \quad \forall m = 1, \dots, M \quad (1)$$

where $h_m(\mathbf{v}) = \mathbf{v}^\top \mathbf{H}_m \mathbf{v}$ for some symmetric measurement matrix $\mathbf{H}_m \in \mathbb{R}^{2N \times 2N}$, and ϵ_m captures the modeling error as well as the measurement noise.

The goal of PSSE is to recover the state vector \mathbf{v} from measurements \mathbf{z} . Specifically, adopting the least-squares criterion and vectorizing the terms in (1), PSSE can be formulated as the following nonlinear least-squares (NLS)

$$\mathbf{v}^* := \arg \min_{\mathbf{v} \in \mathbb{R}^{2N}} \|\mathbf{z} - \mathbf{h}(\mathbf{v})\|^2. \quad (2)$$

A number of algorithms have been advocated for (2), including e.g., Gauss-Newton iterations [2], feasible-point pursuit-based, and semidefinite programming-based solvers in [30], and [38], [14], [17], respectively. Starting from an initial \mathbf{v}_0 , most of these schemes (the former two) iteratively implement a mapping from \mathbf{v}_i to \mathbf{v}_{i+1} , in order to generate a sequence of iterates that hopefully converges to \mathbf{v}^* or some point nearby. In the ensuing subsection, we will focus on the 'workhorse' Gauss-Newton PSSE solver.

A. Gauss-Newton Iterations

The Gauss-Newton method is the most commonly used one for minimizing NLS [19, Sec. 1.5.1]. It relies on Taylor's expansion to linearize the function $\mathbf{h}(\mathbf{v})$. Specifically, at a given point \mathbf{v}_i , it linearly approximates

$$\tilde{\mathbf{h}}(\mathbf{v}, \mathbf{v}_i) \approx \mathbf{h}(\mathbf{v}_i) + \mathbf{J}_i(\mathbf{v} - \mathbf{v}_i) \quad (3)$$

where $\mathbf{J}_i := \nabla \mathbf{h}(\mathbf{v}_i)$ is the $M \times 2N$ Jacobian of \mathbf{h} evaluated at \mathbf{v}_i , with $[\mathbf{J}_i]_{m,n} := \partial h_m / \partial v_n$. Subsequently, the Gauss-Newton method approximates the nonlinear term $\mathbf{h}(\mathbf{v})$ in (2) via (3), and finds the next iterate as its minimizer; that is,

$$\mathbf{v}_{i+1} = \arg \min_{\mathbf{v}} \|\mathbf{z} - \mathbf{h}(\mathbf{v}_i) - \mathbf{J}_i(\mathbf{v} - \mathbf{v}_i)\|^2. \quad (4)$$

Clearly, the per-iteration subproblem (4) is convex quadratic. If matrix $\mathbf{J}_i^\top \mathbf{J}_i$ is invertible, the iterate \mathbf{v}_i can be updated in closed-form as follows

$$\mathbf{v}_{i+1} = \mathbf{v}_i + (\mathbf{J}_i^\top \mathbf{J}_i)^{-1} \mathbf{J}_i^\top (\mathbf{z} - \mathbf{h}(\mathbf{v}_i)) \quad (5)$$

until some stopping criterion is satisfied. In practice however, due to the matrix inversion, the Gauss-Newton method becomes computationally expensive; it also suffers sensitivity to initialization, and it can diverge in certain cases. These limitations prevent its use for real-time monitoring of large-scale networks. To address these challenges, instead of solving every PSSE instance (corresponding to having a new set of measurements in \mathbf{z}) with repeated iterations, an end-to-end approach based on DNNs is pursued next.

III. UNROLLED GAUSS-NEWTON WITH DEEP PRIORS

To mitigate the ill-posedness of PSSE, this section puts forth a flexible topology-aware prior that can be incorporated as a regularizer into standard PSSE tasks such as (2). To solve the resulting regularized PSSE, an alternating minimization-based solver is developed. Later, an end-to-end DNN architecture is constructed by unrolling the alternating minimization solver. Our obtained DNN comprises as building blocks several layers of unrolled Gauss-Newton iterations followed by proximal steps to account for the regularization term. Interestingly, upon utilizing a GNN-based prior, the power network topology can be exploited in PSSE.

A. Regularized PSSE with Deep Priors

In practice, recovering \mathbf{v} from \mathbf{z} is ill-posed, for instance when \mathbf{J}_i is a rectangular matrix. Building on the data-driven deep priors in imaging denoising [26], [3], we advocate regularizing any PSSE loss (here, the NLS in (2)) with some trainable prior information, as follows

$$\min_{\mathbf{v} \in \mathbb{R}^{2N}} \underbrace{\|\mathbf{z} - \mathbf{h}(\mathbf{v})\|^2}_{\text{data consistency}} + \lambda \underbrace{\|\mathcal{P}(\mathbf{v})\|^2}_{\text{regularizer}} \quad (6)$$

where $\lambda \geq 0$ is a tuning hyper-parameter, and regularizer the second term denotes the prior. Similarly to [18], [26], [3], define

$$\mathcal{D}(\mathbf{v}) := (\mathcal{I} - \mathcal{P})(\mathbf{v}) = \mathbf{v} - \mathcal{P}(\mathbf{v}) \quad (7)$$

where \mathcal{I} is the identity operator. Here, the intuition is that $\mathcal{D}(\cdot)$ finds the residual error upon relying on the prior \mathcal{P} . Hence, $\mathcal{P}(\mathbf{v}) = \mathbf{v} - \mathcal{D}(\mathbf{v})$ is the residual error in \mathbf{v} estimate.

Given this interpretation, we propose the following regularized PSSE problem

$$\min_{\mathbf{v} \in \mathbb{R}^{2N}} \|\mathbf{z} - \mathbf{h}(\mathbf{v})\|^2 + \lambda \|\mathbf{v} - \mathcal{D}(\mathbf{v})\|^2. \quad (8)$$

In general, when measurements \mathbf{z} are contaminated by noise or modeling inaccuracies, the second term in (8) will be high. Hence, the regularizer $\|\mathcal{P}(\mathbf{v})\|^2$ encourages solutions that are minimally affected by noise. To encompass a large family of priors, we advocate a DNN-based prior $\mathcal{P}_\theta(\mathbf{v}) = \mathbf{v} - \mathcal{D}_\theta(\mathbf{v})$, where θ collects all the weights of a specified DNN which are to be learned from past data. The DNN $\mathcal{D}_\theta(\cdot)$ can be viewed as a predictor, which, upon taking a Bayesian perspective, generates the posterior mean for a given input.

Although this regularizer promotes desirable properties into PSSE solutions, problem (8) remains nonconvex. In addition, the nested structure of the NN-based regularizer $\mathcal{D}_\theta(\cdot)$ further challenges this problem. Similar to the Gauss-Newton method for NLS in (2), we first develop an alternating minimization algorithm to iteratively approximate the solution of (8). Starting with some initial guess \mathbf{v}_0 , per iteration i uses a linearized data consistency term to compute the next iterate \mathbf{v}_{i+1} ; i.e.

$$\begin{aligned} \mathbf{v}_{i+1} &= \arg \min_{\mathbf{v}} \|\mathbf{z} - \mathbf{h}(\mathbf{v}_i) - \mathbf{J}_i(\mathbf{v} - \mathbf{v}_i)\|^2 + \lambda \|\mathbf{v} - \mathcal{D}_\theta(\mathbf{v}_i)\|^2 \\ &= \mathbf{A}_i \mathbf{z} + \mathbf{B}_i \mathbf{u}_i + \mathbf{b}_i \end{aligned}$$

where the coefficients are given by

$$\mathbf{A}_i := (\mathbf{J}_i^\top \mathbf{J}_i + \lambda \mathbf{I})^{-1} \mathbf{J}_i^\top$$

$$\mathbf{B}_i := \lambda (\mathbf{J}_i^\top \mathbf{J}_i + \lambda \mathbf{I})^{-1}$$

$$\mathbf{b}_i := (\mathbf{J}_i^\top \mathbf{J}_i + \lambda \mathbf{I})^{-1} \mathbf{J}_i^\top (\mathbf{J}_i \mathbf{v}_i - \mathbf{h}(\mathbf{v}_i)).$$

The solution of (6) can thus be approached by alternating between the ensuing two steps

$$\mathbf{u}_i = \mathcal{D}_\theta(\mathbf{v}_i) \quad (10a)$$

$$\mathbf{v}_{i+1} = \mathbf{A}_i \mathbf{z} + \mathbf{B}_i \mathbf{u}_i + \mathbf{b}_i. \quad (10b)$$

Specifically, with initialization $\mathbf{v}_0 = \mathbf{0}$ and input \mathbf{z} , the first iteration yields $\mathbf{v}_1 = \mathbf{A}_0 \mathbf{z} + \mathbf{B}_0 \mathbf{u}_0 + \mathbf{b}_0$. Upon passing \mathbf{v}_1 through the DNN $\mathcal{D}_\theta(\cdot)$, the output \mathbf{u}_1 at the first iteration, which is also the input at the second iteration, is found by (10a). In principle, state estimates can be obtained by repeating these alternating minimizing iterations whenever a new measurement \mathbf{z} becomes available. However, at every iteration i , the Jacobian matrix \mathbf{J}_i must be evaluated, followed by matrix inversions to form \mathbf{A}_i , \mathbf{B}_i , and \mathbf{b}_i . The associated computational burden could be prohibitive for real-time monitoring tasks of large-scale power systems.

For fast implementation, we pursue an end-to-end learning approach that trains a DNN constructed by unrolling iterations of this alternative minimizing solver to approximate directly the mapping from measurements \mathbf{z} to states \mathbf{v} ; see Fig. 1 for an illustration of the resulting GN-DP DNN architecture. Recalling that to derive the alternating minimization solver, the DNN prior $\mathcal{D}_\theta(\cdot)$ in (10a) was assumed pre-trained, with weights θ fixed in advance. In our unrolled GN-DP however, we consider without loss of generality all the coefficients $\{\mathbf{A}_i\}_{i=0}^I$, $\{\mathbf{B}_i\}_{i=0}^I$, $\{\mathbf{b}_i\}_{i=0}^I$, as well as the DNN weights $\{\theta_i\}_{i=0}^I$ to be learnable from data.

This end-to-end GN-DP can be trained using backpropagation using historical or simulated measurement-state training pairs $\{(\mathbf{z}^t, \mathbf{v}^t)\}_{t=1}^T$. Entailing only several matrix-vector multiplications, our GN-DP achieves competitive PSSE performance compared with other iterative solvers such as the Gauss-Newton method. Furthermore, relative to the existing data-driven NN approaches, our GN-DP enjoys avoiding gradients vanishing and exploding, through having direct connections from the input layer to intermediate and output layers (a.k.a skip-connections).

Interestingly, by carefully choosing the specific model for $\mathcal{D}_\theta(\cdot)$, desirable properties such as scalability and high estimation accuracy can be achieved. For instance, if we use feed forward NNs as $\mathcal{D}_\theta(\cdot)$, we can get a scalable solution for large power networks. However, without exploiting the topology of the power grid, feed forward NN is usually physics-agnostic. This prompts us to focus on GNNs, which will capture the topology and physics of the power network. The resultant unrolled Gauss-Newton with GNN priors (GN-GNN) is discussed in details next.

B. Graph Neural Network Deep Prior

To predict state vector \mathbf{v}^* , we model $\mathcal{D}_\theta(\cdot)$ through GNNs, which are known for their rich expressivity. GNNs have recently demonstrated remarkable performance in several tasks, including classification, recommendation, and robotics [15].

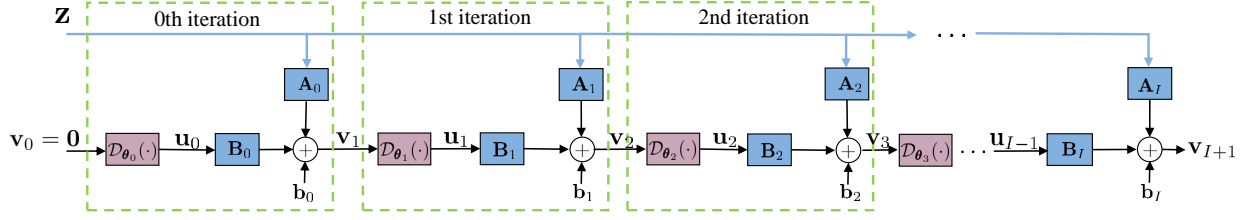


Fig. 1: The structure of the proposed GN-DP.

By operating directly over graphs, GNNs can explicitly leverage the power network topology. Hence, they are attractive options for parameterization in cases where there exists a graph structure [15].

Suppose there is a graph of N nodes associated with a weight matrix \mathbf{W} capturing the connectivity. The GNN takes a signal $\mathbf{X} \in \mathbb{R}^{N \times F}$ as input, whose n -th row $\mathbf{x}_n^\top := [\mathbf{X}]_n$ represents a feature vector of size F for node n . For the PSSE problem at hand, features are real and imaginary parts of the nodal voltage, i.e. $F = 2$. Upon pre-multiplying the input \mathbf{X} by \mathbf{W} , features are propagated over the network, yielding a diffused version $\tilde{\mathbf{Y}} \in \mathbb{R}^{N \times F}$ of the original signal as follows

$$\tilde{\mathbf{Y}} = \mathbf{W}\mathbf{X}. \quad (11)$$

Remark 1. To model feature propagation, a common option is to rely on the adjacency matrix or any other matrix that preserves the structure of the power network (i.e. $\mathbf{W}_{nn'} = 0$ if $(n, n') \notin \mathcal{E}$). Examples include the Laplacian matrix, the random walk Laplacian, and their normalized versions.

Basically, the shift operation in (11) linearly combines the f -th features of all neighbors to obtain its propagated feature. In particular, for a given bus n , the shifted feature $[\tilde{\mathbf{Y}}]_{nf}$ found by

$$[\tilde{\mathbf{Y}}]_{nf} = \sum_{i=1}^N [\mathbf{W}]_{ni} [\mathbf{X}]_{if} = \sum_{i \in \mathcal{N}_n} w_{ni} x_i^f \quad (12)$$

where $\mathcal{N}_n = \{i \in \mathcal{N} : (i, n) \in \mathcal{E}\}$ denotes the set of neighboring buses for bus n . Clearly, this interpretation generates a diffused copy or shift of the signal over the graph.

The convolution operation in GNNs exploits topology information to linearly combine features, namely

$$[\mathbf{Y}]_{nd} := [\mathcal{H} * \mathbf{X}; \mathbf{W}]_{nd} := \sum_{k=0}^{K-1} [\mathbf{W}^k \mathbf{X}]_n : [\mathbf{H}_k]_{:d} \quad (13)$$

where $\mathcal{H} := [\mathbf{H}_0 \dots \mathbf{H}_{K-1}]$ with $\mathbf{H}_k \in \mathbb{R}^{F \times D}$ contains all filter coefficients; $\mathbf{Y} \in \mathbb{R}^{N \times D}$ is the intermediate (hidden) graph signal with D features per bus; and, $\mathbf{W}^k \mathbf{X}$ linearly combines features of buses within the k -hop neighborhood by recursively applying the shift operator \mathbf{W} .

To obtain a GNN with L hidden layers, by abuse of notation, let us now denote by \mathbf{X}_{l-1} the output of the $(l-1)$ -th layer, which is also the input of the l -th layer for $l = 1, \dots, L$, and $\mathbf{X}_0 = \mathbf{X}$ is the input signal. The hidden signal $\mathbf{Y}_l \in \mathbb{R}^{N \times D_l}$

Algorithm 1 PSSE Solver with GNN Priors.

Training phase:

1: **Initialize:**

$$\omega^1 := [\{\Theta_i^1\}_{i=0}^I, \{\mathbf{A}_i^1\}_{i=0}^I, \{\mathbf{B}_i^1\}_{i=0}^I, \{\mathbf{b}_i^1\}_{i=0}^I, \{\mathbf{v}_0^t\}_{t=1}^T].$$

2: **for** $t = 1, 2, \dots, T$ **do**

3: Feed measurements \mathbf{z}^t and \mathbf{v}_0^t into GN-GNN network.

4: **for** $i = 0, 1, \dots, I$ **do**

5: Reshape $\mathbf{v}_i \in \mathbb{R}^{2N}$ to get $\mathbf{X}_0^i \in \mathbb{R}^{N \times 2}$.

6: Feed \mathbf{X}_0^i into GNN.

7: Vectorize the GNN output $\mathbf{X}_L^i \in \mathbb{R}^{N \times 2}$ to get \mathbf{u}_i .

8: Obtain $\mathbf{v}_{i+1} \in \mathbb{R}^{2N}$ using (10b).

9: **end for**

10: Obtain \mathbf{v}_{I+1} using (10b).

11: Minimize the loss $\ell(\mathbf{v}^*, \mathbf{v}_{I+1})$ and update ω^{t+1} .

12: **end for**

Inference phase:

1: **for** $t = T+1, \dots, T'$ **do**

2: Feed real-time measurement \mathbf{z}^t into the trained GN-GNN network.

3: Obtain the estimated voltage \mathbf{v}^t .

4: **end for**

with D_l features is obtained by applying the graph convolution operation (13) at layer l , that is

$$[\mathbf{Y}_l]_{nd} := \sum_{k=0}^{K_l-1} [\mathbf{W}^k \mathbf{X}_{l-1}]_n : [\mathbf{H}_{lk}]_{:g} \quad (14)$$

where $\mathbf{H}_{lk} \in \mathbb{R}^{F_{l-1} \times F_l}$ are the graph convolution coefficients for $k = 0, \dots, K_l - 1$. The output \mathbf{X}_l at layer l is computed by applying a graph convolution followed by a point-wise nonlinear operation $\sigma_l(\cdot)$, such as the rectified linear unit $\sigma_l(t) := \max\{0, t\}$ for $t \in \mathbb{R}$; see Fig. 2 for a depiction. Rewriting (14) in a compact form, we arrive at

$$\mathbf{X}_l := \sigma_l(\mathbf{Y}_l) = \sigma_l\left(\sum_{k=0}^{K_l-1} \mathbf{W}^k \mathbf{X}_{l-1} \mathbf{H}_{lk}\right). \quad (15)$$

The GNN-based PSSE provides a nonlinear functional mapping $\mathbf{X}_L = \Phi(\mathbf{X}_0; \Theta, \mathbf{W})$ that maps the GNN input \mathbf{X}_0 to voltage estimates by taking into account the graph structure through \mathbf{W} , through

$$\Phi(\mathbf{X}_0; \Theta, \mathbf{W}) := \sigma_L\left(\sum_{k=0}^{K_L-1} \mathbf{W}^k \left(\dots \left(\sigma_1\left(\sum_{k=0}^{K_1-1} \mathbf{W}^k \mathbf{X}_0 \mathbf{H}_{1k}\right)\right)\dots\right)\right) \mathbf{H}_{Lk} \quad (16)$$

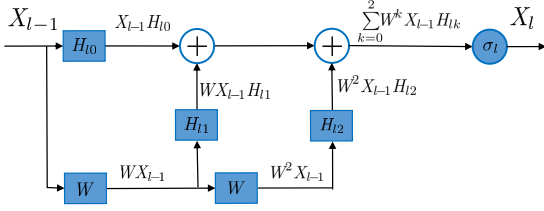


Fig. 2: The signal diffuses from layer $l-1$ to l with $K=3$.

where the parameter set Θ contains all the filter weights; i.e., $\Theta := \{H_{lk}, \forall l, k\}$, and also recall that $X_0 = X$.

Remark 2. With L hidden layers, F_l features and K_l filters per layer, the total number of parameters to be learned is $|\Theta| = \sum_{l=1}^L K_l \times F_l \times F_{l-1}$.

To accommodate the GNN implementation over the proposed unrolled architecture, at the i -th iteration, we reshape the states $v_i \in \mathbb{R}^{2N}$ to an $N \times 2$ matrix, which is the input signal $X_0^i \in \mathbb{R}^{N \times 2}$ to the GNN. Afterwards, we vectorize the GNN output $X_L^i \in \mathbb{R}^{N \times 2}$ to get vector $u_i \in \mathbb{R}^{2N}$ (c.f. (10a)). For convenience, concatenate all trainable parameters of the GN-GNN in vector $\omega := [\{\Theta_i\}_{i=0}^L, \{A_i\}_{i=0}^L, \{B_i\}_{i=0}^L, \{b_i^1\}_{i=0}^L]$, and denote the end-to-end GN-GNN parametric model by $\pi(z; \omega)$, which for given measurements z predicts the voltages across all buses, i.e., $\hat{v} = \pi(z; \omega)$. The GN-GNN weights ω can be updated using backpropagation, upon specifying some loss $\ell(v^*, v_{I+1})$ measuring how well the estimated voltages v_{I+1} by the GN-GNN matches the ground-truth voltages v^* . The proposed method is summarized in Algorithm 1.

IV. ROBUST PSSE SOLVER

In real-time inference, our proposed GN-GNN that has been trained using past data outputs an estimate of the system state vector v^t per slot t from the observed noisy measurements z^t . However, due to impulsive communication noise and cyber-attacks, the proposed GN-GNN may obtain significantly biased estimation results. To accommodate robustness against uncertainties or adversaries, classical formulations including Hüber estimation, Hüber M-estimation, and Schweppe-Hüber generalized M-estimation, consider ϵ -contaminated models for measurements; see e.g., [22], [31]. In contrast, we assume measurements-ground truth voltages are drawn from a nominal yet unknown distribution P_0 , that is $(z, v^*) \sim P_0$. Tying the PSSE problem with distributional assumption, we train the parameters ω upon solving $\min_{\omega} \mathbb{E}_{P_0}[\ell(\pi(z; \omega), v^*)]$ [23]. Note that, in practice only i.i.d. data samples $\{z^t, v^{*t}\}_{t=1}^T \sim \hat{P}_0^{(T)}$ (a.k.a training data) are given and P_0 is unknown. Therefore, a meaningful PSSE solver entails minimizing the empirical loss as follows

$$\min_{\omega} \bar{\mathbb{E}}_{\hat{P}_0^{(T)}}[\ell(\pi(z^t; \omega), v^{*t})] := \frac{1}{T} \sum_{t=1}^T \ell(\pi(z^t; \omega), v^{*t}). \quad (17)$$

To cope with uncertainties and adversaries encountered, robustness can be incorporated into (17), by introducing a set \mathcal{P} of probability distributions that comprises $\hat{P}_0^{(T)}$, and solving the *worst-case* expected loss over the choice of any distribution

satisfying $P \in \mathcal{P}$, which yields the following *distributionally robust* surrogate optimization

$$\min_{\omega} \sup_{P \in \mathcal{P}} \mathbb{E}_P[\ell(\pi(z; \omega), v^*)]. \quad (18)$$

Compared with (17), the worst-case formulation in (18) guarantees reasonable performance across a continuum of distributions in \mathcal{P} . A broad range of ambiguity sets \mathcal{P} can be considered here. Recently, by establishing strong duality conditions for distributionally robust optimization problems using optimal transport theory [28], they have become amongst popular choices to make machine learning models robust [4]. This tractability is the key impetus for this section.

To formalize, consider two probability density functions P and Q defined over a set \mathcal{Z} , and let $\Pi(P, Q)$ be the set of all joint probability distributions defined over \mathcal{Z}^2 , with marginals P and Q . Also $c : \mathcal{Z} \times \mathcal{Z} \rightarrow [0, \infty)$ be a cost function representing the cost of transporting a unit of mass from z in P to another element z' in Q . The so-called optimal transport between two distributions P and Q is given by [28, page 111]

$$W_c(P, Q) := \inf_{\pi \in \Pi} \mathbb{E}_{\pi}[c(z, z')]. \quad (19)$$

Intuitively, $W_c(P, Q)$ denotes the minimum cost associated with transporting all the mass from distribution P to Q . Under some mild conditions over the cost and distributions, the W_c gives the well-known Wasserstein distance between P and Q .

Having introduced distance W_c , let us define the uncertainty set for the given empirical distribution $\hat{P}_0^{(T)}$, as $\mathcal{P} := \{P | W_c(P, \hat{P}_0^{(T)}) \leq \rho\}$ to include all probability distributions having at most ρ -distance from $P_0^{(T)}$. Tying this ambiguity set \mathcal{P} into the generic optimization in (18) yields the following distributionally robust surrogate to arrive at robust PSSE task

$$\min_{\omega} \sup_P \mathbb{E}_P[\ell(\pi(z; \omega), v^*)] \quad (20a)$$

$$\text{s.t. } W_c(P, \hat{P}_0^{(T)}) \leq \rho. \quad (20b)$$

Observe that the inner functional optimization in (20a) runs over all probability distributions P characterized by (20b). Intuitively, solving this optimization directly over the infinite-dimension distribution functions is challenging, if not possible. Fortunately, for continuous loss as well as transportation cost functions, the inner maximization satisfies strong duality condition; that is the optimal objective of this inner maximization and its Lagrangian dual optimal objective are equal. In addition, the dual problem involves optimization over only a one-dimension dual variable. These two observations make it convenient to solve (20) in the dual domain. To formally obtain this tractable surrogate, we call for the following result whose proof can be found in [6].

Proposition 1. Let $\ell : \omega \times \mathcal{Z} \rightarrow [0, \infty)$, and $c : \mathcal{Z} \times \mathcal{Z} \rightarrow [0, \infty)$ satisfy be continuous functions. Then, for any given $\hat{P}_0^{(T)}$, and $\rho > 0$, it holds that

$$\sup_{P \in \mathcal{P}} \mathbb{E}_P[\ell(\pi(z; \omega), v^*)] = \inf_{\gamma \geq 0} \left\{ \bar{\mathbb{E}}_{(z, v^*) \sim \hat{P}_0^{(T)}} \left[\sup_{\zeta \in \mathcal{Z}} \ell(\pi(\zeta; \omega), v^*) + \gamma(\rho - c(z, \zeta)) \right] \right\} \quad (21)$$

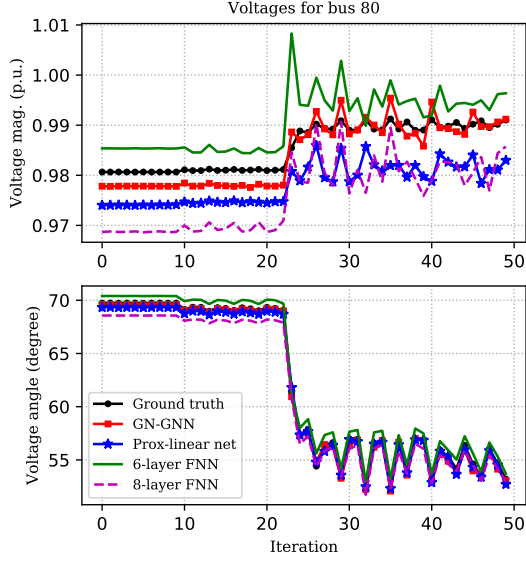


Fig. 3: The estimated voltage magnitudes and angles by the GN-GNN, prox-linear net [36], 6-layer FNN and 8-layer FNN at bus 80 from slots 50 to 100.

where $\mathcal{P} := \{P | W_c(P, \hat{P}_0^{(T)}) \leq \rho\}$.

Remark 3. Thanks to the strong duality, the right-hand side in (21) simply is a univariate dual reformulation of the primal problem represented on the left-hand side. In sharp contrast with the primal formulation, the expectation in the dual domain is taken only over the empirical distribution $\hat{P}_0^{(T)}$ rather than any $P \in \mathcal{P}$. In addition, since this reformulation circumvents the need for finding optimal coupling $\pi \in \Pi$ to define \mathcal{P} , and characterizing the primal objective for all $P \in \mathcal{P}$, it is practically more convenient.

Relying on Proposition 1, we can replace the inner maximization with its dual reformulation to arrive at the following distributionally robust PSSE optimization

$$\min_{\omega} \inf_{\gamma \geq 0} \mathbb{E}_{(z, v^*) \sim \hat{P}_0^{(T)}} \left[\sup_{\zeta \in \mathcal{Z}} \ell(\pi(\zeta; \omega), v^*) + \gamma(\rho - c(z, \zeta)) \right]. \quad (22)$$

Remark 4. Although the robust surrogate in (22) mimics minimax (saddle-point) optimization problems, it requires the supremum to be solved separately per observed measurements z , hence cannot be handled through existing minimax optimization solvers.

It has been shown that under certain mild conditions, with a fixed but appropriately chose γ , one can solve (22) iteratively upon updating ω and maximizing for ζ [27]. Unfortunately, appropriately choosing γ value requires cross validation over a grid search which is also application dependent. Our approach to addressing this, is using a strongly concave function as the transportation cost, such as $c(z, z') := \|z - z'\|_p^2$ for any $p \geq 1$. Then, upon appropriately choosing γ , the inner maximization will have a unique solution, therefore the Dan-

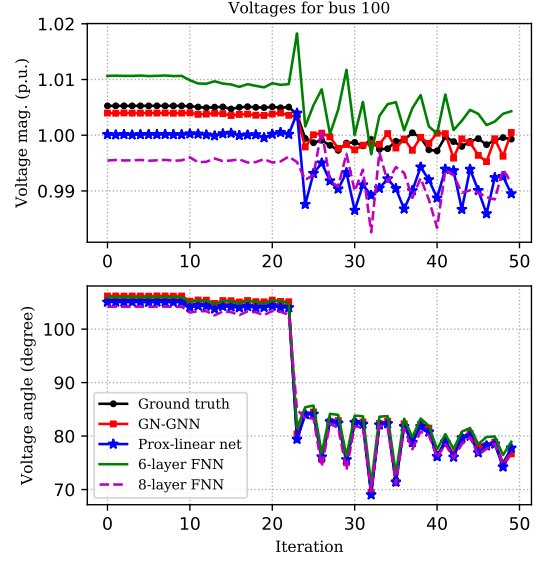


Fig. 4: The estimated voltage magnitudes and angles by the four schemes at bus 100 from slotso 50 to 100.

skin's theorem can be invoked to come up with a differentiable function of ω . As a consequence, we can iteratively solve (22).

Note that having a fixed γ is tantamount to tuning ρ which in turn *controls* the level of *robustness*. Replacing $\gamma \geq 0$ in (22) with a fixed γ , our robust model is this obtained solving

$$\min_{\omega} \mathbb{E}_{(z, v^*) \sim \hat{P}_0^{(T)}} \left[\sup_{\zeta \in \mathcal{Z}} \psi(\omega, \zeta; z, v^*) \right] \quad (23)$$

where

$$\psi(\omega, \zeta; z, v^*) := \ell(\pi(\zeta; \omega), v^*) + \gamma(\rho - c(z, \zeta)). \quad (24)$$

Intuitively, input z in (23) is pre-processed by maximizing $\psi(\cdot)$ which implicitly incorporates robustness against adversaries and uncertainties while training the model.

To robustify the Algorithm 1, we iteratively solve our objective in (23). For a fixed ω^t , and given datum (z^t, v^*) we form $\psi(\cdot)$ (c.f. (24)), implement single gradient ascent as

$$\zeta^t = z^t + \eta^t \nabla_{\zeta} \psi(\omega, \zeta; z^t, v^*)|_{\zeta=z^t} \quad (25)$$

and feed the ζ^t as the input to Algorithm 1. Having observed the loss $\ell(\pi(\zeta^t; \omega^t), v^*)$, we update ω^t using backpropagation.

V. NUMERICAL TESTS

This section the estimation performance as well as robustness of our proposed methods on the IEEE 118-bus benchmark system.

A. Simulation Setup

The simulations were carried out on an NVIDIA Titan X GPU with a 12 GB RAM. For numerical tests, we used real load consumption data from the 2012 Global Energy Forecasting Competition (GEFC) [1]. Using this data, training and testing data were prepared by solving the AC power flow

equations using the MATPOWER toolbox [39]. To match the scale of power demands, we normalized the load data, and fed it into MATPOWER to generate 1,000 pairs of measurements and ground-truth voltages, 80% of which were used for training while the remaining for testing. Measurements include all sending-end active power flows as well as voltage magnitudes, corrupted by additive white Gaussian noise. Standard deviations of the noise added to power flows and voltage magnitudes were set to 0.02 and 0.01 [29], respectively.

A reasonable question to ask is whether explicitly incorporating the power network topology using a trainable regularizer offers improved performance over competing alternatives or not. In addition, it is of interest to study how an adversarial training method enhances the PSSE performance in the presence of bad data and even adversaries. To this aim, three baseline PSSE methods were numerically tested, including: i) the prox-linear network [36]; ii) 6-layer plain-vanilla feed-forward NN (6-layer FNN); and iii) 8-layer feed-forward NN (8-layer FNN). The weights of these NNs were trained using the ‘Adam’ optimizer to minimize the Hübner loss. The learning rate was fixed to 10^{-3} throughout 500 epochs, and the batch size was set to 32.

B. GN-GNN for PSSE

In the first experiment, we implemented a GN-GNN network by unrolling $I = 6$ iterations of the proposed alternating minimizing solver. A GNN with $K = 2$ hops and $D = 8$ hidden units with ReLU activations per unrolled GN-CNN iteration was used for the deep prior. The GN-GNN architecture was designed so that its total number of weight parameters is roughly the same as that of the prox-linear network.

The first set of results depicted in Figs. 3 and 4 show the estimated voltage profiles obtained at buses 80 and 100 from test slots 50 to 100, respectively. The ground-truth and estimated voltages for the first 50 buses on the test slot 100 are presented in Fig. 5. These plots corroborate the competitive or improved performance of the developed GN-GNN relative to the simulated PSSE solvers.

C. Robust PSSE

Despite their remarkable performance in standard PSSE, DNNs may fail to yield meaningful estimates in practice due to bad data. Obviously, this challenges their application in safety-critical power networks. Here, we examine the robustness of our GN-GNN trained with the described adversarial learning method. To this aim, we implemented distributionally robust learning framework to manipulate the input of GN-GNN, prox-linear net, 6-layer FNN, and 8-layer FNN models. Specifically, in distributional attacks, we postulated an ambiguity set \mathcal{P} comprising distributions centered around the nominal data-generating P_0 . Although the training samples were generated according to P_0 , testing samples were obtained using a distribution $P \in \mathcal{P}$ that yields the worst empirical loss. Fig. 6 and 7 demonstrate estimated voltage profiles under distributional attack for a fixed $\gamma = 0.13$ (c.f., (23) and (24)). The plots showcase the robustness of the proposed method against distributional uncertainties, where it outperforms the competing alternatives.

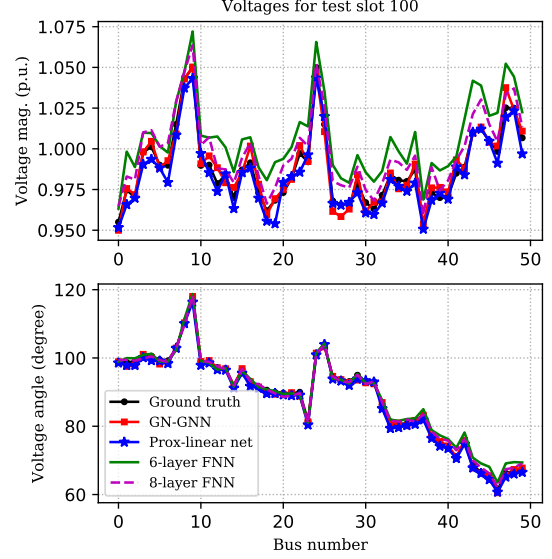


Fig. 5: The estimated voltages magnitudes and angles by the four schemes for the first 50 buses on slot 100.

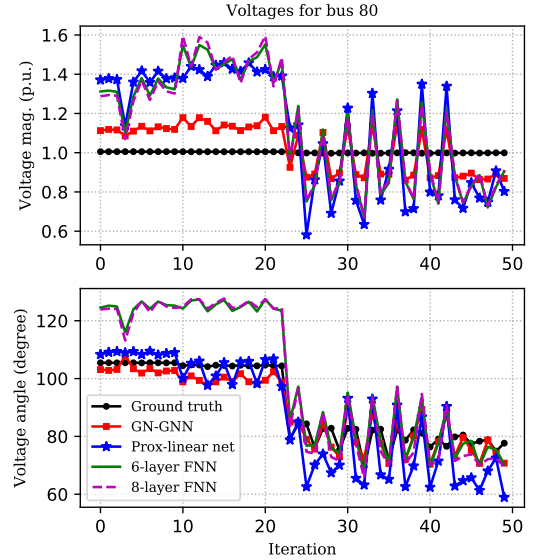


Fig. 6: The estimated voltage magnitudes and angles by the four scheme under distributional attacks at bus 80 from slots 50 to 100.

VI. CONCLUSIONS

This paper advocated topology-aware DNN-based regularizers to address the ill-posedness as well as the nonconvexity of standard PSSE. An alternating minimization solver was developed to approach the solution of the regularized PSSE, which is further unrolled to construct a DNN model. For real-time monitoring of large-scale networks, the resulting DNN was trained using historical or simulated measurement and ground-truth voltages. A basic building block of our GN-GNN consists of a Gauss-Newton iteration followed by a proximal

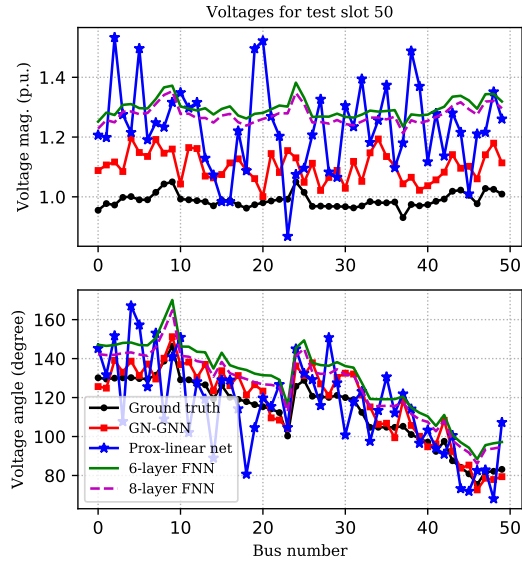


Fig. 7: The estimated voltage magnitudes and under distributional attacks for the first 50 buses on slot 50.

step to deal with the regularization term. Numerical tests showcased the competitive performance of our proposed GN-GNN relative to several existing ones. Further, an adversarial training method was presented to endow the GN-GNN with robustness against bad data. Future directions include exploring such data-driven and topology-aware regularizers for optimal power flow and unit commitment problems.

REFERENCES

- [1] [Online]. Available: <https://www.kaggle.com/c/global-energy-forecasting-competition-2012-load-forecasting/data>.
- [2] A. Abur and A. G. Exposito, *Power System State Estimation: Theory and Implementation*. New York, USA: CRC Press, 2004.
- [3] H. K. Aggarwal, M. P. Mani, and M. Jacob, "MoDL: Model-based deep learning architecture for inverse problems," *IEEE Trans. Med. Imag.*, vol. 38, no. 2, pp. 394–405, Aug. 2018.
- [4] C. Bandi and D. Bertsimas, "Robust option pricing," *Eur. J. Oper. Res.*, vol. 239, no. 3, pp. 842–853, Dec. 2014.
- [5] P. P. Barbeiro, J. Krstulovic, H. Teixeira, J. Pereira, F. J. Soares, and J. P. Iria, "State estimation in distribution smart grids using autoencoders," in *IEEE Intl. Power Engineering and Optimization Conf.*, 2014, pp. 358–363.
- [6] J. Blanchet and K. Murthy, "Quantifying distributional model risk via optimal transport," *Math. Oper. Res.*, vol. 44, no. 2, pp. 565–600, May 2019.
- [7] D. U. Case, "Analysis of the cyber attack on the Ukrainian power grid," *E-ISAC*, vol. 388, Mar. 2016.
- [8] Y. Chen, Y. Shi, and B. Zhang, "Input convex neural networks for optimal voltage regulation," *arXiv:2002.08684*, 2020.
- [9] R. Dobbe, W. Van Westering, S. X. Liu, D. Arnold, D. S. Callaway, and C. Tomlin, "Linear single- and three-phase voltage forecasting and bayesian state estimation with limited sensing," *IEEE Trans. Power Syst.*, vol. 35, no. 3, pp. 1–10, Aug. 2020.
- [10] H. W. Engl, M. Hanke, and A. Neubauer, *Regularization of Inverse Problems*. Berlin, HR: SSBM, 1996, vol. 375.
- [11] P. Fairley, "Cybersecurity at U.S. utilities due for an upgrade: Tech to detect intrusions into industrial control systems will be mandatory," *IEEE Spectr.*, vol. 53, no. 5, pp. 11–13, May 2016.
- [12] X. Hu, H. Hu, S. Verma, and Z.-L. Zhang, "Physics-guided deep neural networks for powerflow analysis," *arXiv:2002.00097*, 2020.
- [13] R. Jabr and B. Pal, "Iteratively re-weighted least absolute value method for state estimation," *IET Gener., Transmiss., Distrib.*, vol. 150, no. 4, pp. 385–391, Jul. 2003.
- [14] M. Jin, J. Lavaei, and K. H. Johansson, "Power grid AC-based state estimation: Vulnerability analysis against cyber attacks," *IEEE Trans. Autom. Contr.*, vol. 64, no. 5, pp. 1784–1799, July 2018.
- [15] T. N. Kipf and M. Welling, "Semi-supervised classification with graph convolutional networks," *arXiv:1609.02907*, 2016.
- [16] A. Kurakin, I. Goodfellow, and S. Bengio, "Adversarial examples in the physical world," *Intl. Conf. Learn. Rep.*, Vancouver, BC, Canada, Apr. 2017.
- [17] Y. Lan, H. Zhu, and X. Guan, "Fast nonconvex SDP solvers for large-scale power system state estimation," *IEEE Trans. Power Syst.*, 2020.
- [18] S. G. Lingala and M. Jacob, "Blind compressive sensing dynamic MRI," *IEEE trans. Med. Imag.*, vol. 32, no. 6, pp. 1132–1145, Mar. 2013.
- [19] O. L. Mangasarian, *Nonlinear Programming*. 2nd ed. Belmont, MA, USA: Athena Scientific, 1999.
- [20] E. Manitsas, R. Singh, B. C. Pal, and G. Strbac, "Distribution system state estimation using an artificial neural network approach for pseudo measurement modeling," *IEEE Trans. Power Syst.*, vol. 27, no. 4, pp. 1888–1896, Nov. 2012.
- [21] H. M. Merrill and F. C. Schweppe, "Bad data suppression in power system static state estimation," *IEEE Trans. Power App. Syst.*, vol. PAS-90, no. 6, pp. 2718–2725, Nov. 1971.
- [22] L. Mili, M. G. Cheniae, and P. J. Rousseeuw, "Robust state estimation of electric power systems," *IEEE Trans. Circuits Syst. I, Fundam. Theory Appl.*, vol. 41, no. 5, pp. 349–358, May 1994.
- [23] D. J. Miller, Z. Xiang, and G. Kesidis, "Adversarial learning targeting deep neural network classification: A comprehensive review of defenses against attacks," *Proc. IEEE*, pp. 1–32, 2020 (To appear).
- [24] J. Ostrometzky, K. Berestizhevsky, A. Bernstein, and G. Zussman, "Physics-informed deep neural network method for limited observability state estimation," *arXiv:1910.06401*, 2019.
- [25] L. I. Rudin, S. Osher, and E. Fatemi, "Nonlinear total variation based noise removal algorithms," *Physica D: Nonlinear Phenomena*, vol. 60, no. 1–4, pp. 259–268, Nov. 1992.
- [26] J. Schlemper, J. Caballero, J. V. Hajnal, A. N. Price, and D. Rueckert, "A deep cascade of convolutional neural networks for dynamic MR image reconstruction," *IEEE Trans. Med. Imag.*, vol. 37, no. 2, pp. 491–503, Oct. 2017.
- [27] A. Sinha, H. Namkoong, and J. Duchi, "Certifying some distributional robustness with principled adversarial training," *Intl. Conf. Learn. Rep.*, Vancouver, BC, Canada, May 2018.
- [28] C. Villani, *Optimal Transport: Old and New*. Berlin, HR: SSBM, 2008, vol. 338.
- [29] G. Wang, G. B. Giannakis, and J. Chen, "Robust and scalable power system state estimation via composite optimization," *IEEE Trans. Smart Grid*, vol. 10, no. 6, pp. 6137–6147, Nov. 2019.
- [30] G. Wang, A. S. Zamzam, G. B. Giannakis, and N. D. Sidiropoulos, "Power system state estimation via feasible point pursuit: Algorithms and cramer-Rao bound," *IEEE Trans. Signal Process.*, vol. 66, no. 6, pp. 1649–1658, Mar. 2018.
- [31] G. Wang, G. B. Giannakis, J. Chen, and J. Sun, "Distribution system state estimation: An overview of recent developments," *Front. Inform. Technol. Electron. Eng.*, vol. 20, no. 1, pp. 4–17, Jan. 2019.
- [32] G. Wu, J. Sun, and L. Xiong, "Optimal switching attacks and countermeasures in cyber-physical systems," *IEEE Trans. Syst., Man, Cybern.: Syst.*, vol. 50, no. 5, pp. 1–10, Jun.
- [33] Q. Yang, G. Wang, A. Sadeghi, G. B. Giannakis, and J. Sun, "Two-timescale voltage control in distribution grids using deep reinforcement learning," *IEEE Trans. Smart Grid*, pp. 1–11, 2019.
- [34] A. Zamzam and K. Baker, "Learning optimal solutions for extremely fast ac optimal power flow," *arXiv preprint arXiv:1910.01213*, 2019.
- [35] A. S. Zamzam and N. D. Sidiropoulos, "Physics-aware neural networks for distribution system state estimation," *arXiv:1903.09669*, 2019.
- [36] L. Zhang, G. Wang, and G. B. Giannakis, "Real-time power system state estimation and forecasting via deep unrolled neural networks," *IEEE Trans. Signal Process.*, vol. 67, no. 15, pp. 4069–4077, Aug. 2019.
- [37] L. Zhang, G. Wang, and G. B. Giannakis, "Real-time power system state estimation via deep unrolled neural networks," in *IEEE Global Conf. on Signal and Info. Process.*, 2018, pp. 907–911.
- [38] H. Zhu and G. B. Giannakis, "Power system nonlinear state estimation using distributed semidefinite programming," *IEEE J. Sel. Topics Signal Process.*, vol. 8, no. 6, pp. 1039–1050, Jun. 2014.
- [39] R. D. Zimmerman, C. E. Murillo-Sanchez, and R. J. Thomas, "MATPOWER: steady-state operations, planning and analysis tools for power systems research and education," *IEEE Trans. Power Syst.*, vol. 26, no. 1, Feb. 2011.